

Hill-Based Model as a Myoprocessor for a Neural Controlled Powered Exoskeleton Arm - Parameters Optimization

Ettore Cavallaro^{1,4}, Jacob Rosen¹, Joel C. Perry², Stephen Burns³, Blake Hannaford¹

¹Department of Electrical Engineering Box 352500

²Department of Mechanical Engineering Box 358725

³Department of Rehabilitation Medicine Box 356490

University of Washington, Seattle WA, 98185, USA

⁴ARTS Lab, Scuola Superiore Sant'Anna, Piazza Martiri della Libertà, 33 - 56127 Pisa, Italy
cavallaro@sss.it, {rosen, jcperry, spburns, blake}@u.washington.edu

Abstract—The exoskeleton robot, serving as an assistive device worn by the human (orthotic), functions as a human-amplifier. Setting the human machine interface (HMI) at the neuro-muscular level may lead to seamless integration and an intuitive control of the exoskeleton arm as a natural extension of the human body. At the core of the exoskeleton HMI there is a myoprocessor. It is a model of the human muscle, running in real-time and in parallel to the physiological muscle, that predicts joint torque as a function of the joint kinematics and neural activation levels. The study is focused on developing a myoprocessor based on the Hill phenomenological muscle model. Genetic algorithms were used to optimize model internal parameters using an experimental database that provides inputs to the model and allows for performance assessment. The results indicate high correlation between joint moment predictions of the model and the measured data. Consequently, the myoprocessor seems an adequate model, sufficiently robust for further integration into the exoskeleton control system.

Index Terms—Exoskeletons, muscle models, genetic algorithms.

I. INTRODUCTION

Integrating human and robot into a single system offers remarkable opportunities for creating a new generation of assistive technology for both healthy and disabled people. Humans possess naturally developed algorithms for control of movement, but have limited muscle strength. Moreover muscle weakness is the primary cause of disability in people with neuromuscular disorders and central nervous system injuries. In contrast, robotic manipulators can perform tasks requiring large forces; however, their artificial control algorithms do not provide the flexibility to perform in a wide range of fuzzy conditions while preserving the same quality of performance as humans. It seems, therefore, that combining the human and the robot into a single integrated system may lead to a solution that will benefit from the advantages offered by each subsystem.

The exoskeleton robot, serving as an assistive device, is worn by the human (orthotic) and functions as a human-amplifier (Fig. 1). Its joints and links correspond to those of the human body, and its actuators share a portion of the

external load with the operator. Setting the human machine interface (HMI) at the neuro-muscular level, using the body's own neural command signals as one of the primary command signals of the exoskeleton, may lead to seamless integration and an intuitive control of the exoskeleton arm as a natural extension of the human body [1], [2].

The neuro-muscular HMI takes advantage of the electro-chemical-mechanical delay (ECMD), an inherent property of the musculoskeletal system. The ECMD exists from the time when the neural system activates the muscular system to the time when the muscles generate moments around the joints. The myoprocessor is a model of the human muscle running in real-time and in parallel to the physiological muscle. During the ECMD, the system will gather information regarding the muscle's neural activation level based on processed signals from surface electromyography (sEMG), joint position, and angular velocity, and will predict the force that will be generated by the muscle before contraction occurs. By the time the human muscles contract, the exoskeleton will move with the human in a synergistic fashion, allowing natural control of the exoskeleton as an extension of the operator's body.

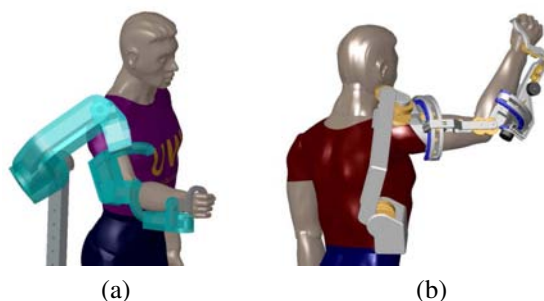


Fig. 1. A 7 DOF Exoskeleton arm: (a) CAD rendering of 7 degrees of freedom (DOF) upper limb powered exoskeleton (shoulder joint - 3 DOF, elbow joint - 1 DOF, wrist joint 3 DOF) (b) An exposed view of the Exoskeleton arm in a reach posture.

The aims of the study are: (i) to develop Hill-based myoprocessors for the flexor/extensor muscles of the elbow joint, (ii) to optimize their parameters using genetic algorithms and (iii) to evaluate the joint-torque moment

predictions of the model with experimental data.

II. MATERIALS AND METHODS

A. Experimental Protocol and Preliminary data processing

The experimental protocol included flexion/extension movements of the elbow joint ($0 - 145^\circ$ range) using the “Arm Curl” VR2 Cybex (Cybex International, Inc) exercise machine (Fig. 2). Each movement was repeated three times with three different loads (4.54, 6.80, 9.07 Kg) moving at three angular velocities (average values of 1.8 ± 0.26 , 1.4 ± 0.13 , 0.7 ± 0.04 rad/s, that are further referred as fast, medium and slow). The joint angle was measured by a potentiometer (Midori America Corp., CA) located on the Cybex machine. sEMG signals were collected using Silver-Silver Chloride surface electrodes (In Vivo Metric) from 28 individual right upper-limb, chest, and back muscles (Fig. 2). Electrodes were located for optimal signal detection based on [3], [4]. Maximal voluntary muscle activations were recorded during isometric contractions. The sEMG signals were amplified by analog amplifiers (Teledyne Inc.) and the data were sampled at 1KHz by a 14 bit A/D card (United Electronic Industries) using the Matlab Real-time workshop toolbox (Mathworks Inc.)

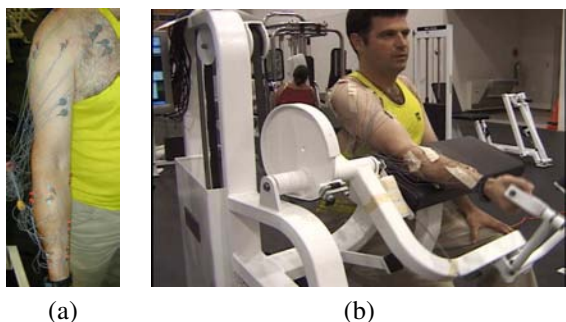


Fig. 2. (a) Surface electrodes attached to the subject measuring EMG signals from 28 muscles simultaneously, (b) Flexing and extending the elbow joint under different loads using CYBEX exercise machine while recording the joint position and muscle EMG signals.

The moments applied on the joint as a function of time by the external load were calculated based on the measured joint kinematics, and the Cybex machine geometry and mechanical model.

B. The myoprocessor

The myoprocessor, depicted in Fig. II-B, is composed of three modules: (i) a module that estimates the degree of neural activation using sEMG signals, (ii) a module that computes the force exerted by the muscle using the activation level and the muscle length and shortening velocity, and (iii) a module that calculates the muscle lengths and moment arms given the joint angles and the limb kinematics. Finally, the torque contribution from each muscle is computed as the product of force and corresponding moment arm.

A Myoprocessor for each one of the seven muscles and sub-muscle groups (head) involved in the flexion/extension

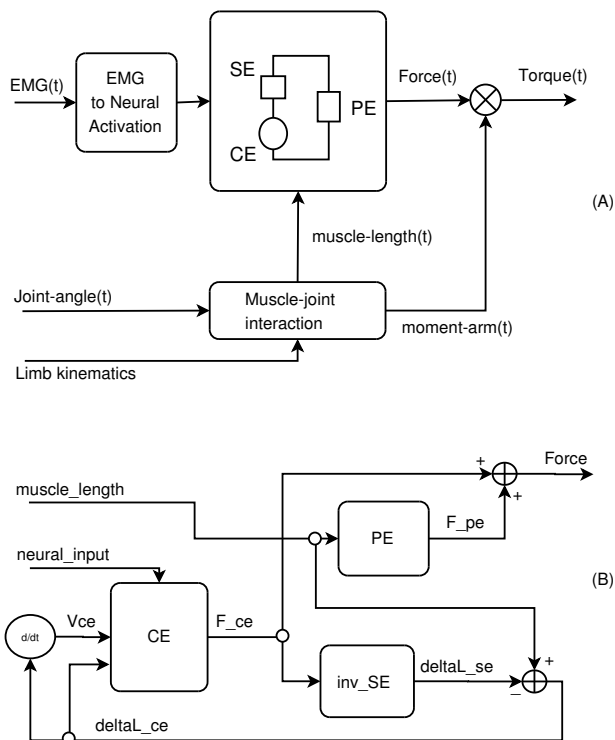


Fig. 3. (A) Myoprocessor Block diagram. (B) Detail of the Hill model implementation (see eq. 1-6); the “inv_SE” block represents eq. 1 solved for ΔL given F_{CE} (that is equal to F_{SE}) as input.

of the elbow joint was implemented in the Matlab/Simulink environment (MathWorks Inc.).

The modeled muscles are: *Brachialis (BRS)*; *Biceps Brachii long head (BLH)*; *Biceps Brachii short head (BSH)*; *Brachioradialis (BRD)*; *Triceps Brachii long head (TLgH)*; *Triceps Brachii medial head (TmH)*; and *Triceps Brachii lateral head (TLtH)*.

The module converting sEMG to neural activation levels consists of a cascade of digital filters (with a causal implementation) and nonlinear blocks: (1) Butterworth 4th order high-pass filter (cut-off frequency 10Hz); (2) Butterworth 4th order notch filter (60 Hz); (3) full wave rectification; (4) Butterworth 4th order low pass filter (cut-off frequency 5 Hz); (5) normalization with respect to the maximal voluntary muscle activation levels [1].

As previously indicated in the literature [5], [6], the moment arm and the length-angle relation have a profound effect on the joint moment prediction. For this reason a model of the muscle-joint interaction based on [7]–[9], has been implemented.

The model in [7]–[9] takes advantage of data derived from the Visible Human Project. For each muscle, origin and insertion points are provided, together with fixed via points, i.e. points that constrain the muscle path. In order to provide better matching with the physiological path, muscles are allowed to wrap around obstacles that simulate other anatomical structures such as muscles, soft tissues, or bones. The obstacles are modeled as spheres, cylinders,

or combination of these two basic elements. The muscle path is then calculated as the shortest path from origin to insertion while maintaining obstacle constraints.

The Hill model of the muscle is a phenomenological model commonly used for its relative computational simplicity. The model presents two elements arranged in series - the passive serial element (SE) and the active contractile element (CE) - and a passive element (PE) arranged in parallel to the previous two. The development of the Hill-based muscle model in this work follows previous research efforts [10]–[12]. An extensive review of literature has been presented by Yarden [12]. The functions describing the three principal elements of the model are defined by Eq. 1-5 [10], [12].

The force generated by PE or SE is defined as

$$F_{PE,SE} = \left[\frac{F_{max}}{e^S - 1} \right] \left[e^{\left(\frac{S}{\Delta L_{max}} \Delta L \right)} - 1 \right] \quad (1)$$

where ΔL is the change in length of the element with respect to the slack length, S is a shape parameter (related to the stiffness of the element), F_{max} is the maximum force exerted by the element for the maximum change in length ΔL_{max} , and $F_{PE,SE}$ is the passive force generated by the PE or the SE element depending on the set of parameters used.

The force generated by the CE element is defined as

$$F_{CE} = u \cdot f_l \cdot f_v \quad (2)$$

$$f_l = \exp \left(-0.5 \left(\frac{\frac{\Delta L_{CE}}{L_{CE_0}} - 0.05}{0.19} \right)^2 \right) \quad (3)$$

$$f_v = \frac{0.1433}{0.1074 + \exp \left(-1.3 \sinh \left(2.8 \frac{V_{CE}}{V_{CE_0}} + 1.64 \right) \right)} \quad (4)$$

$$V_{CE_0} = 0.5(u + 1)V_{CE_{max}} \quad (5)$$

Finally, the total force, F_T , developed by the muscle is:

$$F_T = F_{CE} + F_{PE} \quad (6)$$

In these equations $u \in [0, 1]$ is the normalized neural activation, V_{CE_0} is the maximal CE velocity when $F_{CE} = 0$, f_l is the F_{CE} when $V_{CE} = 0$ and $u = 1$, $V_{CE_{max}}$ is V_{CE_0} when the activation is maximum ($u = 1$), L_{CE_0} is the optimal fiber length.

There are 7 muscles represented in the model, however the sEMG were recorded only from 5 of them due to anatomical limitations in accessing these muscles using non-invasive techniques. In order to estimate the unmeasured neural activation levels, the following assumptions were made: (i) the neural activity of the two heads of the Biceps, measured by a single pair of electrodes, was assumed to be the same except for a scaling factor; (ii) similarly the Brachialis was assigned a scaled version of the Brachioradialis activation level [13], [14].

C. Myoprocessor Parameter Optimization - Genetic Algorithms

A genetic algorithm (GA) was used in order to tune the parameters of the model. GAs are commonly used as optimization techniques [15], [16]. Their advantage over other techniques is in their capability to deal with very large search spaces, minimizing the risk of finding solutions that are only locally optimal. Given an optimization problem, defined by a certain (usually high) number of parameters, GAs find an optimal solution by using simulated evolution processes. The optimal parameters search starts from an initial random population of “chromosomes”, each one representing a potential solution. The “survival of the fittest” criterion and “genetic operators” are used to reach a final population of best solutions [17]. The degree of fitness of a certain set of parameters is evaluated by a problem-specific fitness function. The GA implementation follows a stepwise process:

- 1) Encode the parameters of the problem at hand into a chromosome. Choose an alphabet (such as binary or real numbers) for the genes and choose selection, mutation, crossover, and fitness functions (genetic operators).
- 2) Create the initial population of chromosomes and estimate, using a fitness function, the fitness degree of every chromosome.
- 3) Create an intermediate population, selecting elements from the previous population, using the selection function (a function that privileges best individuals).
- 4) Create new individuals using crossover and mutation and insert them into the population which becomes the new population (“children” substitute “parents” so that population size is stable).
- 5) If the termination criterion is met (i.e., there is an individual whose fitness function has the desired value), terminate evolutive process and give the best individual as result, else start again from step 3.

In this study the chromosome has been designed with 38 “genes”. Each gene represents a scaling factor γ with respect to the reference parameters shown in Table I. A gene with a value of one preserves the reference value of the parameter it represents. For each muscle 5 genes were used with bounded values including: optimal fiber length ($\gamma_{L_{CE_0}} \in [0.8, 1.2]$), maximum force for the optimal fiber length when velocity is zero ($\gamma_{F_{CE_{max}}} \in [0.5, 1.5]$), fast fiber percentage ($\gamma_{\alpha} \in [0.5, 1.5]$), shape factor for PE ($\gamma_{S_{PE}} \in [0.8, 1.2]$), and shape factor for SE ($\gamma_{S_{SE}} \in [0.8, 1.2]$). In addition, three other global parameters were defined: a scale factor for the activation of biceps long head with respect to the short head ($\gamma_{ebi} \in [0.8, 1.2]$), a scale factor Brachialis / Brachioradialis activation level ($\gamma_{ebr} \in [0.5, 4]$) and a geometric scale factor for the skeletal parameters ($\gamma_g \in [0.8, 1.2]$).

The parameters of the model (used in Eq. 1-6) not listed in Table I were computed as follows [12], [5]:

TABLE I
NOMINAL PARAMETERS FOR THE MYOPROCESSOR MODEL BASED ON
[8], [12]

Muscle	L_{max} [cm]	L_{CE_0} [cm]	L_{T_s} [cm]	$F_{CE_{max}}$ [N]	α [%]	S_{PE}	S_{SE}
BSH	40.46	13.07	22.98	461.76	56	9	2.8
BLH	41.94	15.36	22.93	392.91	56	9	2.8
TL _g H	40.29	15.24	19.05	629.21	66	10	2.3
TMH	18.95	4.90	12.19	619.67	66	10	2.3
TL _t H	28.22	6.17	19.64	1268.87	66	10	2.3
BRD	35.35	27.03	6.04	101.58	75	9	2.6
BRA	13.01	10.28	1.75	853.90	38	9	3

$$V_{CE_{max}} = 2 \cdot L_{CE_0} + 8 \cdot L_{CE_0} \cdot \alpha \quad (7)$$

$$F_{PE_{max}} = 0.05 \cdot F_{CE_{max}} \quad (8)$$

$$\Delta_{PE_{max}} = L_{max} - (L_{CE_0} + L_{T_s}) \quad (9)$$

$$F_{SE_{max}} = 1.3 \cdot F_{CE_{max}} \quad (10)$$

$$\Delta_{SE_{max}} = 0.03 \cdot L_{T_s} \quad (11)$$

where α is the percentage of fast fibers in a muscle, L_{T_s} is the tendon slack length (other symbols have been previously defined). Given the experimental protocol, the data collected in one of the repetitions (namely the first repetition, medium velocity, 6.80 Kg load) was used for optimizing the model, whereas the other repetitions were used to evaluate the overall model prediction. In addition, the model predictions were assessed with respect to the actual moments using three criteria: maximum error (Eq. 12), root mean squared error (Eq. 13) and correlation coefficient (Eq. 14). The root mean squared error was also used as a fitness function for the GA.

$$E_{max} = \max_i |T[i] - \tilde{T}[i]| \quad (12)$$

$$E_{rms} = \sqrt{\frac{1}{N} \sum_{i=1}^N (T[i] - \tilde{T}[i])^2} \quad (13)$$

$$\rho = \frac{C_{T\tilde{T}}}{\sigma_T \sigma_{\tilde{T}}} \quad (14)$$

where T represents the actual torque, \tilde{T} is the torque computed by the model, and N is the number of sample points, $C_{T\tilde{T}}$ is the covariance coefficient, σ_T and $\sigma_{\tilde{T}}$ are the standard deviations.

III. RESULTS

Fig. 4 depicts typical kinematics (joint angles), dynamics (joint torques), and the neural activation levels of the flexor/extensor muscles as a function of time. The joint kinematics and the neural activation levels of the muscles were used as inputs to the myoprocessor whereas the external joint load was used to optimize the model parameters and to assess the myoprocessor predictions.

Typical joint torques as a function of time are plotted in Fig. 5. The data depicted represents two repetitions of full flexion/extension of the elbow joint with the following loading conditions: (i) Fig. 5 top - medium velocity, 6.8 Kg - data that were used for optimizing the muscle parameters (ii) Fig. 5 bottom - fast velocity, 9.07 Kg - data that were used to evaluate the myoprocessor predictions. Each plot includes three torques: (1) the actual torque as computed by using the kinematics and the dynamics of the Cybex exercise machine (actual), (2) the myoprocessor predictions with nominal model parameters (non optimized), and (3) with optimized parameters (optimized) using the GA.

The results plotted in Fig. 5 (top) indicate that when comparing the myoprocessor prediction with the actual measured data the maximum error was $E_{max} = 6.5Nm$, the root mean squared error was $E_{RMS} = 2.67Nm$, the correlation coefficient was $\rho = 0.91$, and the excursion, defined as the peak-to-peak amplitude of the torque, was 19.8 Nm. Conversely, the non optimized model yielded $E_{max} = 14.64Nm$, $E_{RMS} = 7.78Nm$, $\rho = 0.79$. The test data set depicted in the bottom plot yielded optimized $E_{max} = 12.6Nm$, $E_{RMS} = 5.2Nm$, $\rho = 0.90$ and non optimized $E_{max} = 23.4Nm$, $E_{RMS} = 11.4Nm$, $\rho = 0.82$.

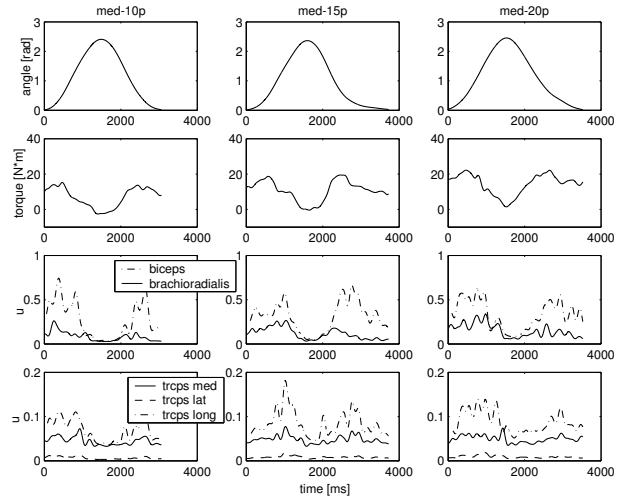


Fig. 4. Typical datasets recorded as part of the experimental protocol for various loading conditions during flexion/extension of the elbow joint.

Table II summarizes the experimental results using the metrics defined in Eq. 12-14. The results were averaged over the two repetitions that were not used for the model optimization.

As part of the optimization process using the GA, the myoprocessor internal parameters deviated from the nominal values presented in table I. Fig. 6 depicts the parameters' scaling factors (nominal values are defined as 0) of all the internal model parameters. This optimal set of parameters (best chromosome) was obtained by using a population of 90 chromosomes and 500 generations. The roulette wheel selection function, together with the elitist method has been used; arithmetic crossover, simple

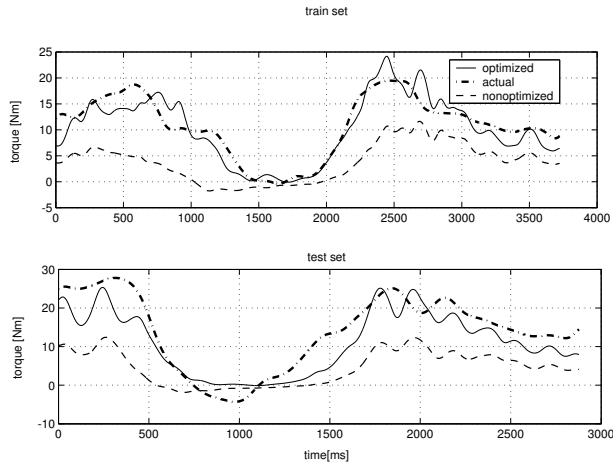


Fig. 5. Actual (dash-dotted), nonoptimized (dashed), and optimized (solid line) moments at the elbow joint during flexion/extension movements as measured and predicted by the myoprocessor. Top panel - the optimization set (medium velocity, 6.8Kg); bottom panel - one of the data sets used for evaluation (fast velocity, 9.07Kg).

TABLE II
AVERAGED RESULTS FOR THE TEST DATA SETS

trial	ρ	E_{rms} [Nm]	E_{max} [Nm]	total excursion [Nm]
fast, 4.54Kg	0.935	4.13	10.20	33.80
fast, 6.80Kg	0.895	4.97	12.85	31.93
fast, 9.07Kg	0.905	5.25	11.95	29.8
med, 4.54Kg	0.855	3.28	14.40	19.72
med, 6.80Kg	0.915	3.41	9.05	27.30
med, 9.07Kg	0.860	6.00	11.40	20.15
slow, 4.54Kg	0.780	3.08	9.78	8.89
slow, 6.80Kg	0.825	4.05	10.28	12.98
slow, 9.07Kg	0.695	7.15	12.30	12.20

crossover, boundary mutation, and uniform mutation have been used as genetic operators [17]. The most significant optimized scaling factors are: (1) the Brachioradialis to Brachialis sEMG scaling factor (~ 3.5); (2) the geometrical scaling factor (~ 1); (3) the maximum force of the three head of the triceps (lowered to the maximum extent); (4) the fast fiber percentage scaling factors (greater than one for all the muscles).

IV. DISCUSSION

The objective of this study was to develop a myoprocessor to be used as an elbow joint moment predictor for an upper limb exoskeleton. As a central element of a neurally controlled exoskeleton, the myoprocessor should be robust, providing accurate torque predictions over broad loading conditions in real-time.

In order to achieve adequate performance and robustness, the myoprocessor has been developed with internal parameters that preserve close ties with the physiological

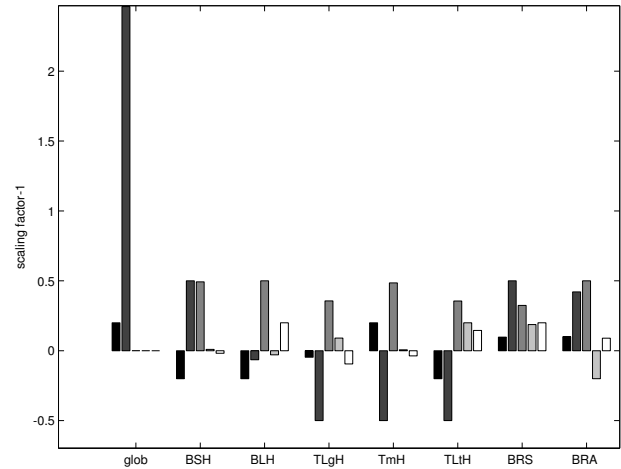


Fig. 6. Scaling factors of the nominal values of the muscle models parameters obtained by the Genetic Algorithm optimization. The nominal values are defined in Table 1. For readability purposes, the scaling factor values present an offset of one. A value of zero indicates that no change was made to the parameter nominal value. The first three genes are 1) scaling factor for biceps long head sEMG, 2) scaling factor for brachialis sEMG, 3) geometrical scaling factor. For each muscle the parameters are: 1) optimal fiber length; 2) maximum force at the optimal length; 3) fast fiber percentage 4) S_{PE} parameter; 5) S_{SE} parameter.

parameters of muscles while preserving the required simplicity to allow real-time operation.

The core of the myoprocessor is a Hill-based muscle model along with a three-dimensional anatomical representation of the upper limb based on the Visible Human Project [7]–[9].

Given the experimental database obtained for various loading conditions, genetic algorithms were used to optimize a large set of the myoprocessor internal parameters. This methodology allows one to modify the generic internal nominal parameters and adjust them to a specific individual under study. As indicated by the results, the ability of the myoprocessors to accurately predict the joint moment increased significantly with an optimized set of internal parameters.

The results indicated that the model is limited in predicting the joint moments for slow movements, particularly when the elbow joint approaches full flexion. This phenomenon could be explained by the lack of measured sEMG data for predicting the Brachialis muscle neural activation levels. In fact, the Brachialis muscle activation levels were estimated as a percentage of the Brachioradialis activation levels [13]. It was previously indicated that the Brachialis is more active during isometric elbow flexion, compared to dynamic elbow flexion, where the biceps plays a major role [14]. When the elbow joint approaches maximum flexion, the moment arm of the Brachialis muscle reaches its maximal value and the joint angular velocity decreases until it reaches a value of zero at the end of the flexion movement.

Therefore it is reasonable to assume that the Brachialis muscle contributes to the overall joint moment. As a result, an approximation of the Brachialis muscle neural

activity based only on the Brachioradialis muscle may lead to some discrepancies in the overall model prediction in these specific conditions. The importance of the Brachialis muscle is confirmed by the relatively high scaling factor value (~ 3.5) obtained with respect to the Brachioradialis muscle. It is also evident that the optimization algorithms tended to lower the maximum force of the Triceps muscle. During the elbow flexion movement the Triceps muscle acts as a joint stabilizer, while decreasing the net joint torque mainly generated by the flexor muscles. Since joint stabilization through co-contraction is not part of the optimization criteria, the optimization process decreases the Triceps muscle contribution to the net joint torque. In future studies more accurate extensor muscle parameters should be obtained by also including active extension movements in the optimization data set.

It is evident from the results (Fig. 6) that no global geometrical scaling was necessary. This result is validated by a close match between the anthropometrical data of the subject under study and the visible human database that was incorporated into the model.

The fast fiber percentage (α) increase that was obtained after the optimization, even if not physiologically satisfactory, could be explained based on the effect it has on $V_{CE_{max}}$ (see eq. 7) and consequently on the shape of the f_v curve (eq. 4). In fact, an increase in α causes an increase in $V_{CE_{max}}$ so that greater values of force could be obtained at a given velocity, during concentric contractions.

Finally, it is worth noticing that the parameters of the model were optimized based on a single data set (repetition #1, medium velocity, 6.8Kg load) and that the model was robust enough to provide adequate predictions while using data sets that were not used for its parameter optimization.

Improvements to the myoprocessor's performance may be obtained in the future by a more refined estimation of the neural activation from the sEMG signals. The muscle model may be refined by using the findings in [18]–[21] that improve the accuracy of the contractile element. In addition a model of the Brachialis muscle activation level may be developed in order to better cope with the lack of noninvasive sEMG data. Finally, the anatomical model of the arm may be refined allowing optimization of all the parameters affecting muscle paths.

In conclusion, the myoprocessor utilizing a Hill-based model provides a robust and accurate prediction of the joint moment given the neural activation levels of the muscles and the joint kinematics. In the future development of this research, one myoprocessor for each muscle of the human arm will be run in real-time (1 KHz) as part of the exoskeleton control system.

ACKNOWLEDGMENT

The authors wish to thank Alex Campbel. As an intern working at the Biorobotics lab - University of Washington he integrated part of the real-time data acquisition system and assisted in the data collections.

REFERENCES

- [1] J. Rosen, M. Brand, M. Fuchs, and M. Arcan, "A myosignal-based powered exoskeleton system," *IEEE Transactions on System Man and Cybernetics - Part A: Systems and Humans*, vol. 31, no. 3, pp. 210–222, 2001.
- [2] J. Rosen, M. B. Fuchs, and M. Arcan, "Performances of hill-type and neural network muscle models - towards a myosignal based exoskeleton," *Computers and Biomedical Research*, 1999.
- [3] J. Basmajian and A. Blumenstien, *Electrode Placement in EMG Biofeedback*. William & Wilkins, 1980.
- [4] J. F. Cram and G. S. Kasman, *Introduction to Surface Electromyography*. Aspen Publishing, 1998.
- [5] J. M. Winters and L. Stark, "Estimated mechanical properties of synergistic muscles involved in movements of a variety of human joints," *Journal of biomechanics*, vol. 21, pp. 1027–1041, 1988.
- [6] M. A. Lemay and P. Crago, "A dynamic model for simulating movements of the elbow, forearm and wrist," *Journal of biomechanics*, vol. 29, pp. 1319–1330, 1996.
- [7] B. A. Garner and M. G. Pandy, "A kinematic model of the upper limb based on the visible human project (vhp) image dataset," *Computer methods in biomechanics and biomedical engineering*, vol. 2, pp. 107–124, 1999.
- [8] B. A. Garner and M. G. Pandy, "Musculoskeletal model of the upper limb based on the visible human male dataset," *Computer methods in biomechanics and biomedical engineering*, vol. 4, pp. 93–126, 2001.
- [9] B. A. Garner and M. G. Pandy, "The obstacle-set method for representing muscle paths in musculoskeletal models," *Computer methods in biomechanics and biomedical engineering*, vol. 3, pp. 1–30, 2000.
- [10] J. M. Winters, *Multiple muscle systems: biomechanics and movement organization*, ch. Hill based muscle models: a system engineering perspective, pp. 69–93. Springer-Verlag, N.Y., 1990.
- [11] F. E. Zajac, "Muscles and tendons: properties, models, scaling, and application to biomechanics and motor control," *Critical Reviews in Biomedical Engineering*, 1989.
- [12] O. Yarden, *Dynamics of racket-arm interaction applied to "tennis elbow"*. PhD thesis, University of Tel-Aviv, 1996.
- [13] T. S. Buchanan, G. P. Rovai, and W. Z. Rymer, "Strategies for muscle activation during isometric torque generation at the human elbow," *J Neurophysiol*, 1989.
- [14] A. A. Tax, J. J. D. van der Gon, C. C. Gielen, and C. M. V. den Tempel, "Differences in the activation of m. biceps brachii in the control of slow isotonic movements and isometric contractions," *Exp Brain Res*, 1989.
- [15] J. Holland, *Adaptation In Natural and Artificial Systems*. The University of Michigan Press, Ann Arbour, 1975.
- [16] Z. Michalewicz, *Genetic algorithms + data structures = Evolution programs*. Springer, 1996.
- [17] C. R. Houk, J. A. Joines, and M. G. Kay, "A genetic algorithm for function optimization: a matlab implementation," tech. rep., North Carolina State University, 1995.
- [18] I. E. Brown and G. E. Loeb, "Measured and modeled properties of mammalian skeletal muscle. i. the effects of post-activation potentiation on the time course and velocity dependencies of force production," *Journal of Muscle Research and Cell Motility*, 1999.
- [19] I. E. Brown, E. J. Cheng, and G. E. Loeb, "Measured and modeled properties of mammalian skeletal muscle. ii. the effects of stimulus frequency on force-length and force-velocity relationships," *Journal of Muscle Research and Cell Motility*, 1999.
- [20] I. E. Brown and G. E. Loeb, "Measured and modeled properties of mammalian skeletal muscle. iii. the effects of stimulus frequency on stretch-induced force enhancement and shortening-induced force depression," *Journal of Muscle Research and Cell Motility*, 2000.
- [21] I. E. Brown and G. E. Loeb, "Measured and modeled properties of mammalian skeletal muscle. iv. dynamics of activation and deactivation," *Journal of Muscle Research and Cell Motility*, 2000.